

EXPLORING MULTI-SENSOR SATELLITE SYNERGIES TO PROVIDE DIRECTION TO HIGH-RESOLUTION ALONG-TRACK ALTIMETRY CURRENTS

Francesco Nencioli, Graham Quartly, and Peter Miller

Plymouth Marine Laboratory, United Kingdom

ABSTRACT

A new approach to compute along-track velocity components by combining altimetry-based across-track components and front directions from remote sensing maps of surface chlorophyll concentration is proposed. The analysis focuses on the South Madagascar region characterized by the strong East Madagascar Current and sharp gradients of surface tracers. The results are compared against in-situ observations from three moorings along the Jason-1 track 196. Accurate information on the total velocity direction is the key factor for obtaining accurate estimates of along-track velocities. Although with some limitations, surface tracer fronts can be successfully used to retrieve such information.

Key words: Satellite synergy; Along-track currents; Ocean Color CCI; East Madagascar Current.

1. INTRODUCTION

In the last two decades, satellite altimetry has emerged as one of the main tools for the investigation of surface ocean dynamics. Multiple altimeter observations can be combined to produce global maps of surface velocities capable of resolving structures of the order of 100 km. However, they cannot provide information at smaller scales (the meso- and sub-mesoscale, from 100 to 10 of km), which in recent years have been recognised to be critical for the ocean energy budget and global biogeochemical cycles. Along track observations, on the other hand, are characterized by higher resolution than the gridded products and therefore have the potential to provide information on (sub)mesoscale dynamics. Their main limitation is that they can only provide estimates of the velocity component perpendicular to the track. Methods based on multi-sensor satellite synergies represent one of the most promising approaches for retrieving high-resolution two-dimensional velocities.

Here we propose an approach that combines the directional information retrieved from satellite observations of surface ocean tracers (such as ocean colour and sea surface temperature) with sea level altimetry to retrieve the

total surface velocities along the altimeter track. This work has been developed within the context of Globcurrent, an ESA-funded project that specifically aims at “advancing the quantitative estimations of ocean surface currents from satellite sensor synergies”.

2. DATA AND METHODS

As surface tracers are continuously stirred by ocean circulation, their fields are characterized by fronts predominantly aligned with the direction of the dominant currents. Based on this, the approach we propose in this study uses the front directions from maps of chlorophyll concentration, α_{front} (here defined as the angle between a chlorophyll front and the across-velocity vector), to retrieve the along-track velocity components, V_{along} , associated with each altimetry-based across-track velocity, V_{cross} . In particular, V_{along} is computed as

$$V_{along} = V_{cross} \tan(\alpha_{front}) \quad (1)$$

so that the resulting total velocity vector, \mathbf{V} , will have direction parallel to the front and the same across-track component as measured from altimetry. α_{front} varies between -90 and 90 degrees, so that for the same front the sign of V_{along} is automatically determined by that of V_{cross} (i.e. for a negative α_{front} , V_{along} is positive(southward) when V_{cross} is negative(westward), and vice-versa).

This study focuses on the South Madagascar region, which presents favourable characteristics for testing our approach (Figure 1). In particular, these include: *a*) the East Madagascar Current (EMC), an intense poleward flow that is almost perpendicular to the Jason-1 196 satellite track (hereafter J1-196); *b*) strong surface tracer gradients; *c*) 3 moorings deployed from February 2005 to April 2006 along the J1-196 track, which provide the velocity observations for validating our results.

The analysis is based on the AVISO/DUACS 2014 filtered altimetry data collected along the J1-196 track from February 2005 to April 2006. The data have spatial resolution of 14 km and temporal resolution of 10 days. V_{cross} components have been computed from along-track absolute dynamic topography using a 3rd order, 3-point

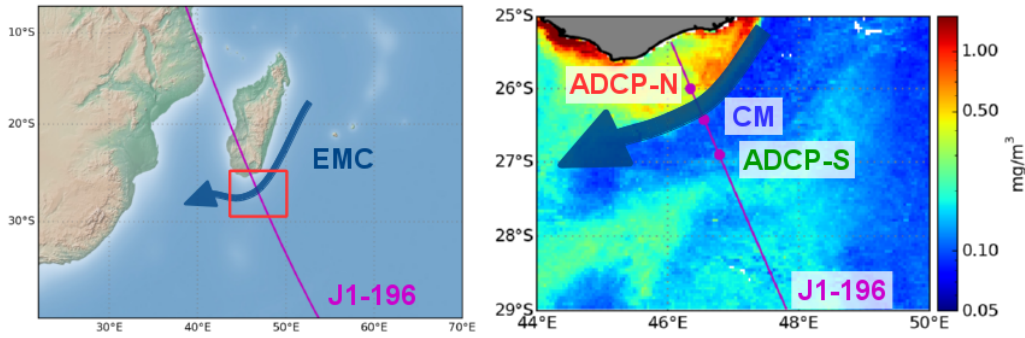


Figure 1. (Left) Geographical map of the Madagascar region with the position of the East Madagascar Current and the Jason-1 track 196 indicated. The red rectangle marks the region of focus of this study. (Right) 7-day composite map of surface chlorophyll concentration for the region of study. EMC, J1-196 and the positions of the three moorings (ADCP-N, CM and ADCP-S) are also indicated.

stencil centre differencing. 7-day composite maps of surface chlorophyll concentration based on the Ocean Color CCI dataset (4 km spatial resolution) were computed for each day that altimetry data are available. The maps were obtained by averaging all the observations available for each pixel within 3 days before and 3 days after the date of each J1-196 passage. Using 7-day composites drastically reduced the number of missing pixels due to cloud coverage on each map and, at the same time, only moderately smoothed the main chlorophyll patterns which preserved their general shape and direction.

The three moorings were deployed at $46^{\circ}21'E$, $26^{\circ}00'S$ (ADCP-N), $46^{\circ}33'E$, $26^{\circ}25'S$ (CM) and $46^{\circ}47'E$, $26^{\circ}54'S$ (ADCP-S). ADCP-N and ADCP-S were both equipped with upward-facing Acoustic Doppler Current Profilers (ADCP) 75kHz at 500 m depth. CM included an RCM 11 discrete self-recording current meter. All moorings provided time-series of hourly measurements of velocity at ~ 140 m depth. The time-series were moving averaged with a Gaussian window with full width at half maximum (FWHM) of 6 inertial periods (one inertial period ranges between 26 and 27 hours at the mooring latitudes) to remove the signal associated with high-frequency processes, such as tidal and inertial motions. Comparison between the averaged time-series of V_{cross} from the moorings and those from remote sensing shows a good fit (correlation coefficient $r=0.88$, not shown). Mooring velocities are usually weaker than the ones from remote sensing, most likely due to the depth difference between the two measurements.

3. COMPUTING ALONG-TRACK COMPONENTS

The first step of the analysis consisted in estimating the direction of the chlorophyll fronts. The 7-day composite maps of chlorophyll concentration were used to retrieve the spatial distribution of the total chlorophyll gradients. The gradients were computed from the base 10 logarithm of chlorophyll concentration. This allowed the

reliable identification not only of the strong gradients between coastal and open ocean waters at the southern tip of Madagascar, but also of the open ocean gradients characterized by much lower chlorophyll variations. The gradient fields were smoothed with a 2-dimensional Gaussian moving average filter (FWHM of ~ 40 km) to reduce the noise and highlight the gradients associated with the main patterns of surface chlorophyll. Estimates of α_{front} were directly derived from those fields as the perpendicular direction to the total gradients (Figure 2, top right). Values of the total gradient and the associated α_{front} at the locations of each altimetry observation along the J1-196 track were then obtained through nearest neighbor interpolation. These were combined with the satellite V_{cross} to compute V_{along} using equation 1 (Figure 2, bottom).

Comparison between the reconstructed \mathbf{V} vectors and the satellite-based V_{cross} shows that although in most cases the direction of \mathbf{V} seems to better match the underlying patterns of chlorophyll concentration, there are situations where the \mathbf{V} vectors show unrealistic patterns (Figure 2, top left). In particular, strong reconstructed velocities, often arranged in sequences of diverging/converging vectors, can occur when α_{front} is almost parallel to the satellite track (e.g. at $46^{\circ}20'E$, $26^{\circ}S$ and $47^{\circ}E$, $27^{\circ}20'S$ in Figure 2, top right). Such features are associated with contours of the weaker (compared to across-stream ones) down-stream gradients of chlorophyll concentrations. Thus, α_{front} resulting from such gradients should not be used to derive V_{along} from equation 1, since it assumes tracer isolines parallel to velocity directions.

The relation between large reconstructed V_{along} and α_{front} is further confirmed by Figure 3. In particular, the scatter plot shows how as α_{front} increases (i.e. as fronts become progressively more and more parallel to the satellite track) it is more and more likely to obtain anomalously high values of V_{along} . This is a direct consequence of the reconstructed V_{along} being proportional to $\tan(\alpha_{front})$ in equation 1. Tangent values rapidly increase above the unity between 50 and 65° , so that the reconstructed V_{along} for α_{front} of 50 , 57.5 and 65° are respectively 1.19, 1.57 and 2.14 times larger than satellite

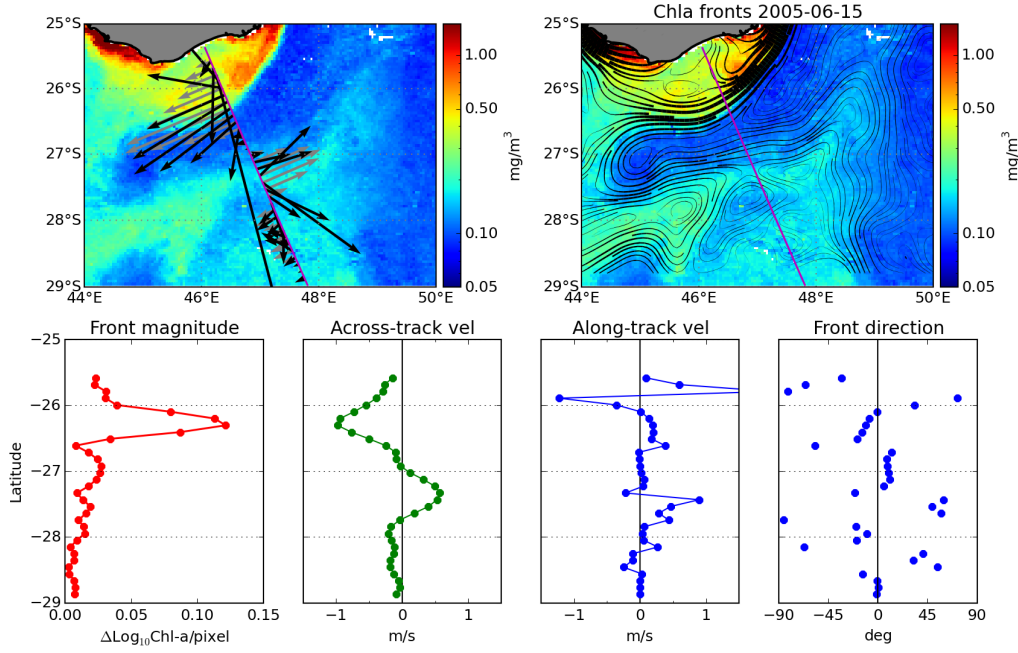


Figure 2. (Top left) Cross-track, V_{cross} , and reconstructed total velocities, \mathbf{V} , (grey and black vectors, respectively) superimposed on the 7-day composite map of chlorophyll concentration for June 15, 2005. (Top right) Same chlorophyll map with superimposed the contourlines indicating the direction of the chlorophyll fronts. The thickness of the lines is proportional to the magnitude of the total gradient. (Bottom left to right) Along-track front magnitude, satellite across-track velocities (V_{cross}), estimated along-track velocities (V_{along}) and front directions (α_{front}). Along-track velocities are obtained by combining across-track velocities and front directions using equation 1.

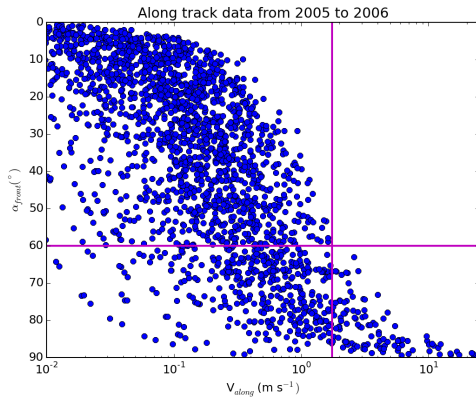


Figure 3. Scatter plot of reconstructed V_{along} magnitude (in \log_{10} scale) and corresponding α_{front} direction. Magenta lines indicate $V_{along} = 1.75 \text{ m s}^{-1}$ and $\alpha_{front} = 60^\circ$.

V_{cross} . With maximum values of satellite V_{cross} on the order of 1 m s^{-1} , this implies reconstructed V_{along} ranging from 1.2 to more than 2 m s^{-1} . Indeed, the analysis indicates $|\alpha_{front}| = 60^\circ$ as the threshold beyond which reconstructed $V_{along} > 1.75 \text{ m s}^{-1}$ (used here as a conservative threshold for unrealistic values) are obtained.

Based on these observations, to mitigate the presence of artifacts in the reconstructed V_{along} , we decided to base

our analysis only on the strongest fronts with absolute $\alpha_{front} < 60^\circ$. The strongest fronts were identified as along-track local maxima (within an interval of 70 km, corresponding to 5 successive observations) of the total gradient magnitude (Figure 4, bottom left). In case the maxima were associated with absolute $\alpha_{front} > 60^\circ$, a default value of 60° was used instead. To compute V_{along} , it was then necessary to interpolate between the values associated with the strongest fronts to reconstruct the full along-track profile of α_{front} .

Before the interpolation, information from the satellite V_{cross} was also integrated in the analysis. In particular, as the region is mainly characterized by alternating currents of opposite direction and almost perpendicular to the J1-196 track, the points of zero-crossing of satellite V_{cross} (Figure 4, bottom centre-left) were used to define the positions at which $\alpha_{front} = 0^\circ$ (i.e. current direction perpendicular to the satellite track; Figure 4 bottom right). This constraint enabled the reconstruction of more accurate α_{front} along-track profiles, since it strongly reduced the magnitude of the divergence/convergence within the region of shear between opposite currents. As velocities within those regions are usually small, even in case currents are not exactly perpendicular to the satellite track, inaccuracies introduced by imposing slightly different directions at the zero-crossing did not result in large errors on the reconstructed V_{along} . The full profile of α_{front} was then computed by interpolating the values associated with either front maxima or V_{cross} zero-crossings. As a

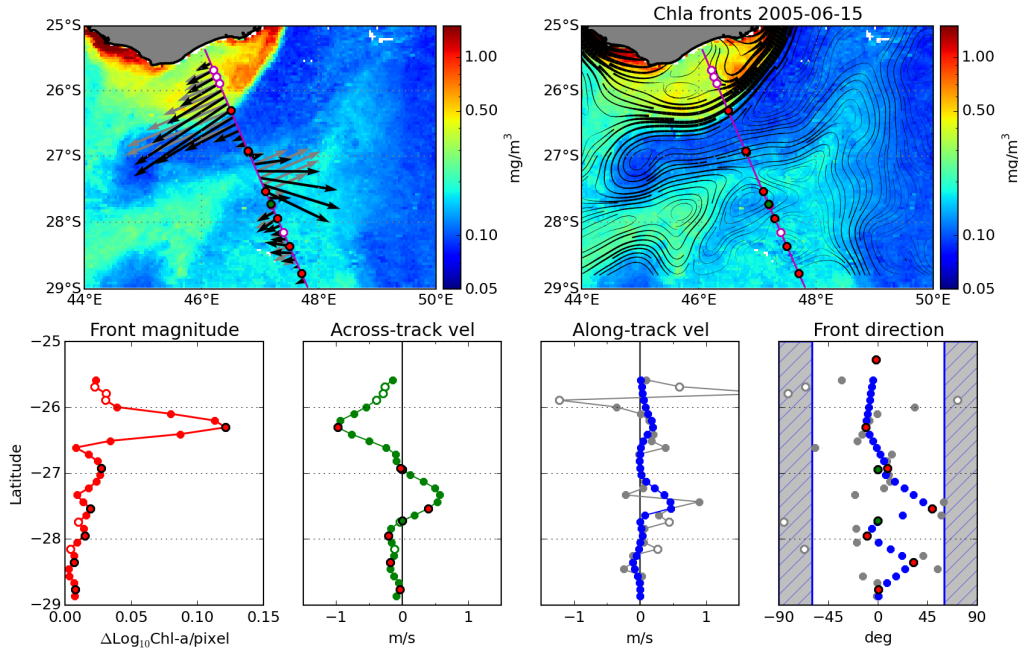


Figure 4. (Top left) Cross-track, V_{cross} , and reconstructed total velocities from the interpolated front directions, \mathbf{V} , (grey and black vectors, respectively). As in Figure 2, these are superimposed on the 7-day composite map of chlorophyll concentration for June 15, 2005. The circles along the J1-196 track indicate the position of: local maxima of front intensity (red); points of across-track velocity crossing (green); absolute front directions larger than 60° (white). This is valid for all panels in the figure. (Top right) Same as Figure 2. (Bottom left to right) Same as Figure 2. In the centre-right and right panels, V_{along} from original and interpolated α_{front} , and original and interpolated α_{front} are in grey and blue, respectively. Shaded areas in the right panel mark the boundaries where absolute values of $\alpha_{front} > 60^\circ$.

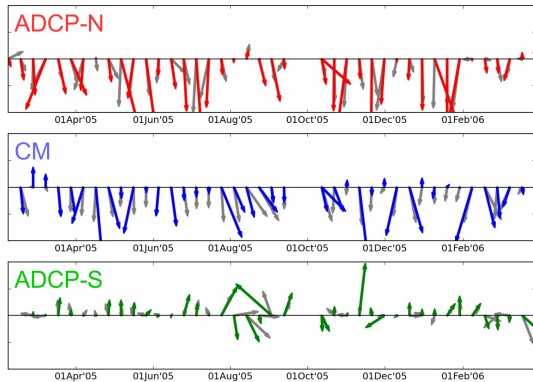


Figure 5. Time series of measured and reconstructed \mathbf{V} vectors (gray and colour, respectively) at the three mooring sites. The x-axis is parallel to the satellite track with the North to the left.

first test, we decided to use a simple linear interpolation (Figure 4 bottom right).

The interpolated along-track profile of α_{front} was used to compute new estimates of V_{along} (Figure 4, bottom centre-right). As shown by the plot, the along-track distribution of the new V_{along} is not characterized by the unrealistic spikes obtained using the original α_{front} profile. Moreover, the resulting \mathbf{V} vectors (Figure 4, top left)

are not affected by patterns of divergence/convergence as in Figure 2, while at the same time they remain consistent with the structures shown by the underlying surface chlorophyll field.

4. COMPARISON WITH IN-SITU OBSERVATIONS

A more quantitative evaluation of the performances of our approach was obtained by directly comparing the reconstructed V_{along} with the ones directly measured at the three mooring sites (Figure 5). As expected, the in-situ observations show that V_{along} are weaker than V_{cross} , confirming that in the region of study currents are predominantly zonal with directions nearly perpendicular to the J1-196 track. The reconstructed values of V_{along} are within the range of the mooring observations. The three time series show some periods of good agreement between reconstructed and observed velocities (e.g. Mar-Apr 2005 and after Feb-Mar 2006 for the ADCP-N and CM time series), as well as periods of poor agreement (e.g. Aug-Sep 2005 and Mar-Apr 2006 for the ADCP-S time series). In general, when the analysis provided accurate estimate of α_{front} , the resulting reconstructed velocities are accurate. Periods when the analysis performances are poor, are usually characterized by: a) weak satellite V_{cross} (with directions often opposite to the in-

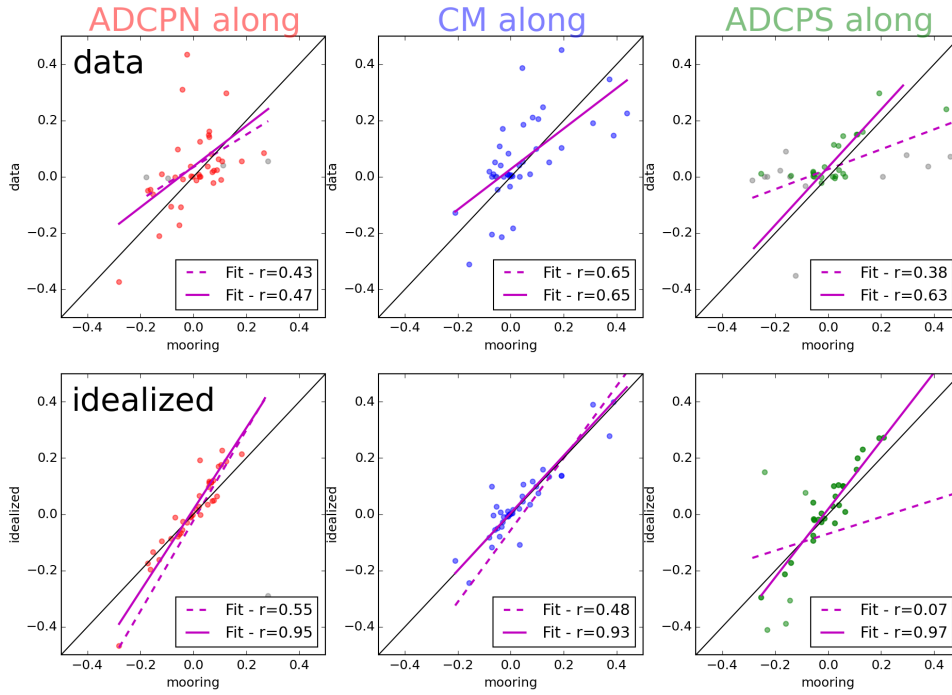


Figure 6. Correlations between observed and reconstructed V_{along} for the three moorings. (Top row) V_{along} computed using satellite V_{cross} and α_{front} . (Bottom row) V_{along} computed using satellite V_{cross} and in-situ α_{front} . Dashed magenta lines represent the linear fits using all data; solid magenta lines represent the fits discarding the data with observed velocity direction $> 60^\circ$ (grey circles). Values of the correlation coefficients (r) are indicated in each panel.

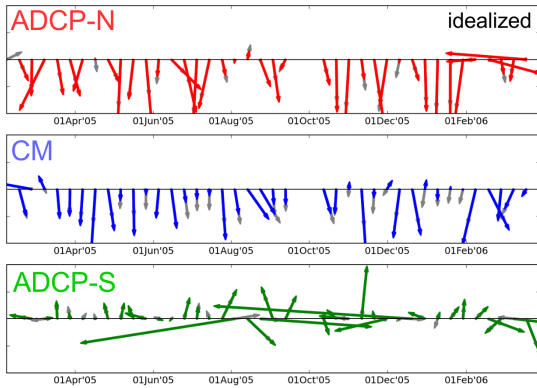


Figure 7. Same as Figure 5. The reconstructed velocity vectors are obtained combining satellite V_{cross} and idealized V_{along} computed using the observed velocity directions.

situ ones); b) in-situ velocities almost parallel to the satellite track (in-situ $\alpha_{front} > 60^\circ$).

Correlations between observed and reconstructed V_{along} for the three moorings (Figure 6, top row) show that the best fit occurs for CM ($r=0.65$). Among the three moorings, CM is the closest to the average location of the strong chlorophyll front between coastal and open ocean waters, and thus it is likely to be characterized by the most accurate estimates of α_{front} . On the other hand, the worst fit occurs for the ADCP-S mooring ($r=0.38$).

The mooring is located in a region often characterized by recirculation structures associated with weaker velocities intersecting the J1-196 track at higher angles than at the other two sites. Also, some of the surface circulation might be decoupled from that at 140 m.

To assess the quality of those fits, we have computed V_{along} substituting the α_{front} from satellite tracer observations in equation 1 with the direction of the in-situ velocities. Since these V_{along} are derived with perfect knowledge of the velocity directions, their correlations with the observed ones represent an ideal test to evaluate the best possible fits that could be achieved using the synergy between across-track velocities and directional information from surface tracer observations. Indeed, the correlations for the three moorings (Figure 6, bottom row) show that in all cases ideal and in-situ data are well aligned along the 1:1 line. At the same, that is not the case for the computed correlation lines, which results in relatively low values of the correlation coefficients. Such low values occur due to a sporadic unreasonably high values of V_{along} (out of scale in the plot) which are obtained also in the idealized case with perfect knowledge of velocity direction. As in the case of satellite-based V_{along} (Figure 6, top row), the ADCP-S mooring is the one characterized by the worst performances.

To understand why such big values of V_{along} occur, we compared again the time-series of the observed and reconstructed V vectors for the three mooring sites (Figure 7). This time, the reconstructed vectors are ob-

tained combining satellite V_{cross} and idealized V_{along} . The three time series show that even with perfect knowledge of the velocity direction, bad agreement between observed and reconstructed velocities occur in case of: *a)* satellite V_{cross} with opposite direction from the observed ones (e.g. Aug 2005 for the ADCP-S time series); *b)* observed velocities almost parallel to the satellite tracks (e.g. Mar 2006 for the ADCP-N time series; Sep-Dec 2005 for the ADCP-S one). Indeed, even in the idealized case, unrealistic values of $V_{along} > 1.75 \text{ m s}^{-1}$ are obtained when the direction of the observed velocities is $> 60^\circ$.

By removing the high values of V_{along} obtained for such high directions, the fits for the idealized case in Figure 6 drastically improve: the computed correlations lines become more aligned with the 1:1 line (even though as in the case of V_{cross} , in-situ velocities are characterized by slightly lower values than satellite ones) and the correlation coefficients jump to 0.95, 0.93 and 0.97 for the ADCP-N, CM and ADCP-S moorings, respectively (Figure 6, bottom row). However, when doing the same for the V_{along} obtained from the analysis, the fits do not show similar improvements, and the correlation coefficients remain 0.47, 0.65 and 0.63 (Figure 6, top row).

5. CONCLUSIONS

The results of our study show that accurate knowledge of total velocity direction is the key factor to successfully retrieve along-track velocities from synergy between along-track altimetry and remote sensing surface tracer observations. Information on total velocity direction can be successfully obtained from the direction of surface tracer front. However, not all front directions can be used in the analysis: high front angles and contouring features of the total gradient fields can lead to unrealistic patterns of reconstructed V_{along} characterized by large velocities and strong divergence/convergence. The most reliable information on velocity directions is provided by the strongest fronts. To compute V_{along} , the full along-track profile of α_{front} needs to be reconstructed from those directions. Linear interpolation between the local maxima of front direction provides only moderately successful results. Therefore, alternative methods to propagate the directional information along the whole track should be explored in future studies. With this perspective, it is important to remark that in some situation (i.e. bad satellite V_{cross} directions, velocities almost parallel to the satellite track) retrieving along-track velocities will always be problematic, even with perfect knowledge of velocity direction.